Three-dimensional Green's functions in anisotropic magneto-electro-elastic bimaterials

Ernian Pan

Abstract. In this paper, we derive three-dimensional Green's functions in anisotropic magneto-electro-elastic full space, half space, and bimaterials based on the extended Stroh formalism. While in the full space, the Green's functions are obtained in an explicit form, those in the half space and bimaterials are expressed as a sum of the full-space Green's function and a Mindlin-type complementary part, with the latter being evaluated in terms of a regular line integral over $[0, \pi]$. Despite the complexity involved, the current Green's function expressions are surprisingly simple. Furthermore, the piezoelectric, piezomagnetic, and purely elastic Green's functions can all be obtained from the current Green's functions by setting simply the appropriate material coefficients to zero. A special material case, to which the extended Stroh formalism cannot be applied directly, has also been identified.

Simple numerical examples are presented for Green's functions in full space, half space, and bimaterials with fully coupled and uncoupled anisotropic magneto-electro-elastic material properties. For given material properties and fixed source and field points, the effect of magneto-electro-elastic coupling on the Green's function is discussed. In particular, we observed that magneto-electro-elastic coupling could significantly alter the magnitude of certain Green's displacement and stress components, with difference as high as 45% being noticed. This result is remarkable and should be of great interest in the material analysis and design.

Keywords. Green's functions, magneto-electro-elastic solids, 3D bimaterials, anisotropy, Stroh formalism.

Introduction

Owing to their special features like lightweight and high strength, composite materials are nowadays applied to various areas of science and engineering. More recent advances are the smart or intelligent materials where piezoelectric and/or piezomagnetic materials are involved. These materials have the ability of converting energy from one form to the other (among magnetic, electric, and mechanical energies). Furthermore, composites made of piezoelectric/piezomagnetric materials exhibit magnetoelectric effect that is not present in single-phase piezoelectric or piezomagnetic materials [1,2].

In order to study the behavior of composites under various loading situations, some analytical, experimental, and numerical approaches have been proposed.

Among the numerical approaches, both the finite element method (FEM) and the boundary element method (BEM) have received special attention due to their flexibility and feasibility to various numerical problems. The BEM is becoming attractive, as it requires discretization of the problem boundary only, offering certain computational advantages over the domain discretization methods. In applying the BEM, however, the so-called kernel functions (i.e., Green's functions, or fundamental solutions, or singular solutions) need to be given. For the piezoelectric case, Green's functions in two-dimensional (2D) and three-dimensional (3D) full spaces and bimaterials have all been investigated and derived [3-6]. While the piezomagnetic Green's functions can be directly obtained from the piezoelectric Green's functions by simply replacing the piezoelectric constants with the piezomagnetic constants, 3D Green's functions in a composite made of piezoelectric/piezomagnetic materials, either in a full space or bimaterials, have never been derived.

Besides its indispensable to the BEM, the Green's function also has wide application in micromechanics and material sciences, as reviewed in the article by Bacon et al. [7] and documented in the book by Mura [8]. Recent advances in this area are on the study of various inclusion-related problems in piezoelectric/piezomagnetic materials [1,2, 9-13]. In general, these analyses are in terms of the well-known Eshelby tensor [8], which is, in general, directly related to the Green's functions.

The Stroh formalism has been found to be mathematically elegant and numerical powerful to handle problems in anisotropic materials [3]. Ting [14] reviewed recent development of the Stroh formalism in applied mechanics and predicted the potential application of this method to various 3D problems. It is true that very complicated 2D problems can be treated using the Stroh formalism, even for the magneto- electro-elastic media [15-18]. Yet, no Green's functions are available in the literature for the corresponding 3D magneto-electro-elastic media. With regard to the 3D anisotropic elastic material, there are only a few papers in the literature using the Stroh formalism [14], starting from the classic solution for the surface Green's displacements on an anisotropic half space by Barnett and Lothe [19]. After more than twenty years, Ting and Lee [20] derived and discussed the 3D Green's functions in an anisotropic full space, and Wu [21] derived the corresponding full-space and half-space Green's functions, both in terms of the Stroh formalism. Stimulated by these significant advances, Pan and Yuan [5,6] have been able to derive the 3D bimaterial Green's functions in both anisotropic elastic and piezoelectric media. Again the elegant Stroh formalism was used in the procedure of their derivation. What makes these Green's functions most attractive is that the Green's functions are expressed as a sum of a Kelvin-type solution and a Mindlin-type part. While the Kelvin-type solution is singular but in an analytical form, the Mindlin-type part is expressed in terms of a regular line integral over a finite interval [5,6].

As a continuous devotion to the research along this line, in this paper we present the 3D Green's functions in general anisotropic magneto-electro-elastic full space, half space and bimaterials. To derive the Green's functions in 3D full space, we make use of the Radon transform to reduce the problem to a Cauchy integral with the pole being the eigenvalues of the Stroh formalism. Therefore, an analytical and explicit expression is obtained for the 3D Green's function in general anisotropic magneto-electro-elastic full space. For the bimaterial case, with half space being a special case, we first applied the 2D Fourier transform to the equations of equilibrium to arrive at an extended Stroh formalism in the transformed domain, assuming that the involved Stroh eigenvalues are all complex. When inverting back to the physical domain, we introduced a polar coordinate transform to get rid of the infinite integral. Finally, we are able to express the bimaterial Green's functions in terms of a full-space part or the Kelvin-type solution and a complementary part or the Mindlin-type part [22]. Therefore we further demonstrate that the Stroh formalism can equally and successfully be applied to the [3D] anisotropic piezoelectric/piezomagnetic bimaterials.

Numerical examples are also presented for full-space, half-space, and bimaterial domains with fully coupled and uncoupled anisotropic magneto-electro-elastic material properties. For the given material properties, the effects of magnetoelectricity and of problem domains (full space, half-space, and bimaterials) on the extended Green's displacements and stresses are clearly observed. In particular, we noticed that for the given source and field points and material properties, the coupling effect of magnetoelectricity on the Green's displacements and stresses can be as high as 40%, a new phenomenon never being reported before.

While the Green's functions derived in this paper can be directly applied to some micromechanics-related problems (opening, inclusion, eigenstrain, etc.) in smart and composite material analysis and design, relatively complicated structure problems can be solved using the boundary integral equation method with the current solutions being served as the integral kernels.

Basic equations

Using the extended Barnett and Lothe notation [23], the equations of equilibrium for the coupled magneto-electro-elastic media can be expressed as [9,12,15,17]:

$$C_{iJKl}, u_{K,li} + f_J = 0 \qquad (1)$$

In this paper, summation from 1 to 3 (1 to 5) over repeated lowercase (uppercase) subscripts is assumed, and a subscript comma denotes the partial differentiation with respect to the coordinates (i.e., x_1, x_2, x_3 or x, y, z). In equation (1), the

extended displacement and *extended* body force are defined as

$$u_I = \begin{cases} u_i & I = 1,2,3 \\ \phi & I = 4 \\ \psi & I = 5 \end{cases} \quad ; \quad f_J = \begin{cases} f_j & J = 1,2,3 \\ -f_e & J = 4 \\ -f_m & J = 5 \end{cases} \tag{2}$$

Where u_i, ϕ, and ψ are the elastic displacement, electric potential, and magnetic potential, respectively; f_i, f_e, and f_m are the body force, electric charge, and electric current (or called magnetic charge as compared to the electric charge), respectively.

The *extended* elastic coefficient tensor C_{iJKl} in equation (1) relates the *extended* strains to the *extended* stresses by the constitutive relation

$$\sigma_{iJ} = C_{iJKl}\gamma_{Kl} \tag{3}$$

where the extended stresses and strains are defined by

$$\sigma_{iJ} = \begin{cases} \sigma_{ij} & J = 1,2,3 \\ D_i & J = 4 \\ B_i & J = 5 \end{cases} \quad ; \quad \gamma_{Ij} = \begin{cases} \gamma_{ij} & I = 1,2,3 \\ -E_j & I = 4 \\ -H_j & I = 5 \end{cases} \tag{4}$$

and the extended elastic coefficient tensor has the following components

$$C_{iJKl} = \begin{cases} C_{ijkl} & J,K = 1,2,3 \\ e_{lij} & J = 1,2,3; \ K = 4 \\ e_{ikl} & J = 4; \ K = 1,2,3 \\ q_{lij} & J = 1,2,3; \ K = 5 \\ q_{ikl} & J = 5; \ K = 1,2,3 \\ -\lambda_{il} & J = 4; \ K = 5 \text{ or } J = 5; \ K = 4 \\ -\varepsilon_{il} & J,K = 4 \\ -\mu_{il} & J,K = 5 \end{cases} \tag{5}$$

In equations (4) and (5), σ_{ij}, D_i, and B_i are the stress, electric displacement, and magnetic induction (i.e., magnetic flux), respectively; γ_{ij}, E_i, and H_i are the strain, electric field and magnetic field, respectively; C_{ijlm}, ε_{ij}, and μ_{ij} are the elastic, dielectric, and magnetic permeability tensors, respectively; e_{ijk}, q_{ijk}, and λ_{ij} are the piezoelectric, piezomagnetic, and magnetoelectric coefficients, respectively. It is observed that various uncoupled cases can be reduced from equations (1)-(5) by setting the appropriate coefficients to zero, which will be investigated later. It is further noticed that the following symmetry relations hold:

$$\begin{aligned} C_{ijlm} &= C_{jilm} = C_{lmij} \\ e_{kji} &= e_{kij}; \ q_{kji} = q_{kij} \\ \varepsilon_{ij} &= \varepsilon_{ji}; \ \lambda_{ij} = \lambda_{ji}; \ \mu_{ij} = \mu_{ji} \end{aligned} \tag{6}$$
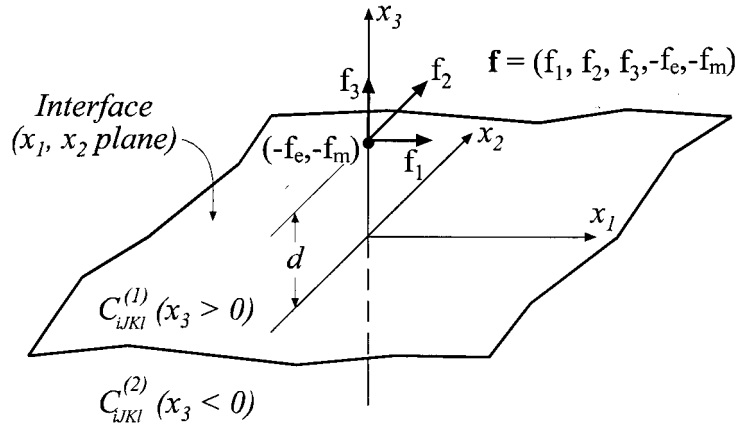
Figure 1.
An anisotropic magneto-electro-elastic bimaterial full-space subjected to an extended concentrated force $\mathbf{f}(f_1, f_2, f_3, -f_e, -f_m)$ applied at $(0, 0, d)$ in material 1.

Finally, the *extended* strains and displacements are related by

$$\gamma_{ij} = \frac{1}{2}(u_{i,j} + u_{j,i})$$
$$E_i = -\phi_{,i}; \ H_i = -\psi_{,i}$$

(7)

In the following sections, we will use the *extended displacement* to stand for the elastic displacement, electric, and magnetic potentials, as defined in equation (2), and the *extended stress* for the stress, electric displacements, and magnetic induction as defined in equation (4).

It is observed that the structures of equations (1) and (3) are similar to their purely elastic and piezoelectric counterparts. Therefore, the solution method developed recently by Pan and Yuan [5,6] will be adopted and applied to derive the Green's functions in general anisotropic magneto-electro-elastic materials.

Problem description

We consider an anisotropic magneto-electro-elastic bimaterial full-space where $x_3 > 0$ and $x_3 < 0$ are occupied by materials 1 and 2, respectively (Figure 1), with the interface being at $x_3 = 0$ plane. Without loss of generality, we assume that an extended concentrated force $\mathbf{f} = (f_1, f_2, f_3, -f_e, -f_m)$ is applied at $(0, 0, d)$ in material 1 with $d > 0$.

The continuity conditions at the interface $x_3 = 0$ require that the extended displacement and traction vectors are continuous, with the later, named $\mathbf{t}$, being

defined by

$$\mathbf{t} = (\sigma_{31}, \sigma_{32}, \sigma_{33}, D_3, B_3) \tag{8}$$

At the plane $x_3 = d$ where the extended point force is applied, the extended displacement vector is continuous while the extended traction vector experiences a jump across the $x_3 = d$ plane, with the magnitude equal to the extended point force. Besides these continuity conditions, the solutions in the regions of $x_3 > d$ and $x_3 < 0$ are required to vanish as x_3 approaches $+\infty$ and $-\infty$, respectively.

Stroh formalism and general solutions in the transformed domain

Similar to the purely elastic and/or piezoelectric bimaterial problems [5,6], we apply the two-dimensional Fourier transforms

$$\tilde{u}_K(y_1, y_2, x_3) = \int \int u_k(x_1, x_2, x_3) e^{i(y_1 x_1 + y_2 x_2)} dx_1 dx_2 \tag{9}$$

to equation (1). Therefore in the transformed domain, this equation, in the absence of the extended force, becomes

$$C_{\alpha I K \beta} y_\alpha y_\beta \tilde{u}_K + i(C_{\alpha I K 3} + C_{3IK\alpha}) y_\alpha \tilde{u}_{K,3} - C_{3IK3} \tilde{u}_{K,33} = 0 \tag{10}$$

where $\alpha, \beta = 1, 2$. Now, letting

$$\begin{bmatrix} y_1 \\ y_2 \\ 0 \end{bmatrix} = \eta\mathbf{n}, \quad \mathbf{n} = \begin{bmatrix} n_1 \\ n_2 \\ 0 \end{bmatrix} = \begin{bmatrix} \cos\theta \\ \sin\theta \\ 0 \end{bmatrix}, \quad \mathbf{m} = \begin{bmatrix} 0 \\ 0 \\ 1 \end{bmatrix} \tag{11}$$

a general solution of equation (10) can then be expressed as

$$\tilde{\mathbf{u}}(y_1, y_2, x_3) = \mathbf{a} e^{-ip\eta x_3} \tag{12}$$

with p and $\mathbf{a}$ satisfying the following extended eigenrelation:

$$[\mathbf{Q} + p(\mathbf{R} + \mathbf{R}^T) + p^2 \mathbf{T}]\mathbf{a} = 0 \tag{13}$$

where

$$Q_{IK} = C_{jIKs} n_j n_s, \quad R_{IK} = C_{jIKs} n_j m_s, \quad T_{IK} = C_{jIKs} m_j m_s \tag{14}$$

and the superscript T denotes the matrix transpose. Equation (13) is the extended magneto-electro-elastic Stroh eigenrelation in the oblique plane spanned by $\mathbf{n}$ and $\mathbf{m}$ defined in equation (11), a direct extension of the elastic and piezoelectric Stroh eigenrelation. Similar to the elastic and piezoelectric cases [3,24], it can be show that the eigenvalues of equation (13) are either complex or purely imaginary (by

requiring a positive internal energy for the system). Once the eigenvalue problem (13) is solved, the extended displacements in the Fourier transformed domain are then obtained from equation (12).

In order to find the extended stresses in the Fourier transformed domain, we start with the physical domain relation. In the physical domain, the extended traction vector $\mathbf{t}$ on the $x_3 = $ constant plane and the extended in-plane stress vector $\mathbf{s}$ are related to the extended displacements as

$$\mathbf{t} = (C_{31Kl}u_{K,l}, C_{32Kl}u_{K,l}, C_{33Kl}u_{K,l}, C_{34Kl}u_{K,l}, C_{35Kl}u_{K,l}) \tag{15}$$

$$\mathbf{s} \equiv (\sigma_{11}, \sigma_{12}, \sigma_{22}, D_1, D_2, B_1, B_2)$$
$$= (C_{11Kl}u_{K,l}, C_{12Kl}u_{K,l}, C_{22Kl}u_{K,l}, C_{14Kl}u_{K,l}, C_{24Kl}u_{K,l}, C_{15Kl}u_{K,l}, C_{25Kl}u_{K,l}) \tag{16}$$

Taking the Fourier transform, we then find that the transformed extended traction and in-plane stress vectors can be expressed as

$$\tilde{\mathbf{t}} = -i\eta\mathbf{b}e^{-ip\eta x_3} \tag{17}$$

$$\tilde{\mathbf{s}} = -i\eta\mathbf{c}e^{-ip\eta x_3} \tag{18}$$

with

$$\mathbf{b} = (\mathbf{R}^T + p\mathbf{T})\mathbf{a} = -\frac{1}{p}(\mathbf{Q} + p\mathbf{R})\mathbf{a}$$
$$\mathbf{c} = \mathbf{H}\mathbf{a} \tag{19}$$

where the matrix $\mathbf{H}$ is defined by

$$\mathbf{H} = \begin{bmatrix} C_{111\alpha}n_\alpha + pC_{1113} & C_{112\alpha}n_\alpha + pC_{1123} & C_{113\alpha}n_\alpha + pC_{1133} & C_{114\alpha}n_\alpha + pC_{1143} & C_{115\alpha}n_\alpha + pC_{1153} \\ C_{121\alpha}n_\alpha + pC_{1213} & C_{122\alpha}n_\alpha + pC_{1223} & C_{123\alpha}n_\alpha + pC_{1233} & C_{124\alpha}n_\alpha + pC_{1243} & C_{125\alpha}n_\alpha + pC_{1253} \\ C_{221\alpha}n_\alpha + pC_{2213} & C_{222\alpha}n_\alpha + pC_{2223} & C_{223\alpha}n_\alpha + pC_{2233} & C_{224\alpha}n_\alpha + pC_{2243} & C_{225\alpha}n_\alpha + pC_{2253} \\ C_{141\alpha}n_\alpha + pC_{1413} & C_{142\alpha}n_\alpha + pC_{1423} & C_{143\alpha}n_\alpha + pC_{1433} & C_{144\alpha}n_\alpha + pC_{1443} & C_{145\alpha}n_\alpha + pC_{1453} \\ C_{241\alpha}n_\alpha + pC_{2413} & C_{242\alpha}n_\alpha + pC_{2423} & C_{243\alpha}n_\alpha + pC_{2433} & C_{244\alpha}n_\alpha + pC_{2443} & C_{245\alpha}n_\alpha + pC_{2453} \\ C_{151\alpha}n_\alpha + pC_{1513} & C_{152\alpha}n_\alpha + pC_{1523} & C_{153\alpha}n_\alpha + pC_{1533} & C_{154\alpha}n_\alpha + pC_{1543} & C_{155\alpha}n_\alpha + pC_{1553} \\ C_{251\alpha}n_\alpha + pC_{2513} & C_{252\alpha}n_\alpha + pC_{2523} & C_{253\alpha}n_\alpha + pC_{2533} & C_{254\alpha}n_\alpha + pC_{2543} & C_{255\alpha}n_\alpha + pC_{2553} \end{bmatrix} \tag{20}$$

with $\alpha = 1, 2$. Therefore, once all the eigenvectors $\mathbf{a}_m$ are found, the Green's functions in the Fourier-transformed domain are completely known, the beauty of the Stroh formalism.

If p_m, $\mathbf{a}_m$, and $\mathbf{b}_m$ ($m = 1, 2, \ldots 10$) are the eigenvalues and the associated eigenvectors, we let

$$\text{Im} p_J > 0, \ p_{J+5} = \bar{p}_J, \ \mathbf{a}_{J+5} = \bar{\mathbf{a}}_J, \ \mathbf{b}_{J+5} = \bar{\mathbf{b}}_J \ (J = 1, 2, 3, 4, 5)$$
$$\mathbf{A} = [\mathbf{a}_1, \mathbf{a}_2, \mathbf{a}_3, \mathbf{a}_4, \mathbf{a}_5], \ \mathbf{B} = [\mathbf{b}_1, \mathbf{b}_2, \mathbf{b}_3, \mathbf{b}_4, \mathbf{b}_5], \ \mathbf{C} = [\mathbf{c}_1, \mathbf{c}_2, \mathbf{c}_3, \mathbf{c}_4, \mathbf{c}_5, \mathbf{c}_6, \mathbf{c}_7] \tag{21}$$

where Im stands for the imaginary part and the overbar denotes the complex conjugate. Assuming that p_J are distinct, and the eigenvectors $\mathbf{a}_J$, and $\mathbf{b}_J$ satisfy the following normalization relation [3,19]

$$\mathbf{b}_I^T \mathbf{a}_J + \mathbf{a}_I^T \mathbf{b}_J = \delta_{IJ} \tag{22}$$

with δ_{IJ} being the Kronecker delta of 5×5, then the general solutions of equation (12) in the transformed domain can be obtained by superposing the ten eigensolutions of equation (13), that is

$$\begin{aligned}
\tilde{\mathbf{u}}(y_1, y_2, x_3) &= i\eta^{-1}\bar{\mathbf{A}}\langle e^{-i\bar{p}_* \eta x_3}\rangle \bar{\mathbf{q}} + i\eta^{-1}\mathbf{A}\langle e^{-ip_* \eta x_3}\rangle \mathbf{q}' \\
\tilde{\mathbf{t}}(y_1, y_2, x_3) &= \bar{\mathbf{B}}\langle e^{-i\bar{p}_* \eta x_3}\rangle \bar{\mathbf{q}} + \mathbf{B}\langle e^{-ip_* \eta x_3}\rangle \mathbf{q}' \\
\tilde{\mathbf{s}}(y_1, y_2, x_3) &= \bar{\mathbf{C}}\langle e^{-i\bar{p}_* \eta x_3}\rangle \bar{\mathbf{q}} + \mathbf{C}\langle e^{-ip_* \eta x_3}\rangle \mathbf{q}'
\end{aligned} \tag{23}$$

where $\bar{\mathbf{q}}$ and $\mathbf{q}'$ are arbitrary complex vectors to be determined and

$$\langle e^{-ip_* \eta x_3}\rangle = \mathrm{diag}[e^{-ip_1 \eta x_3}, e^{-ip_2 \eta x_3}, e^{-ip_3 \eta x_3}, e^{-ip_4 \eta x_3}, e^{-ip_5 \eta x_3}] \tag{24}$$

It is noteworthy that, besides their obvious dependence on material properties, the matrices $\mathbf{A}$, $\mathbf{B}$, $\mathbf{C}$, vectors $\bar{\mathbf{q}}$, $\mathbf{q}'$, and p_J are also functions of the unit vector $\mathbf{n}$.

Bimaterial Green's functions in the transformed domain

Using the transformed continuity (or jump) and finiteness conditions for the extended displacement and traction vectors, the magneto-electro-elastic bimaterial Green's functions in the transformed domain can be derived similar to the purely elastic and piezoelectric cases [5,6]. For $x_3 > d$ (in material 1):

$$\begin{aligned}
\tilde{\mathbf{u}}_1(y_1, y_2, x_3) &= -i\eta^{-1}\bar{\mathbf{A}}_1\langle e^{-i\bar{p}_*^{(1)}\eta(x_3-d)}\rangle \bar{\mathbf{q}}_1^\infty - i\eta^{-1}\bar{\mathbf{A}}_1\langle e^{-ip_*^{(1)}\eta(x_3-d)}\rangle \bar{\mathbf{q}}_1 \\
\tilde{\mathbf{t}}_1(y_1, y_2, x_3) &= -\bar{\mathbf{B}}_1\langle e^{-i\bar{p}_*^{(1)}\eta(x_3-d)}\rangle \bar{\mathbf{q}}_1^\infty - \bar{\mathbf{B}}_1\langle e^{-ip_*^{(1)}\eta(x_3-d)}\rangle \bar{\mathbf{q}}_1 \\
\tilde{\mathbf{s}}_1(y_1, y_2, x_3) &= -\bar{\mathbf{C}}_1\langle e^{-i\bar{p}_*^{(1)}\eta(x_3-d)}\rangle \bar{\mathbf{q}}_1^\infty - \bar{\mathbf{C}}_1\langle e^{-ip_*^{(1)}\eta(x_3-d)}\rangle \bar{\mathbf{q}}_1
\end{aligned} \tag{25}$$

For $0 \leq x_3 < d$ (in material 1):

$$\begin{aligned}
\tilde{\mathbf{u}}_1(y_1, y_2, x_3) &= i\eta^{-1}\bar{\mathbf{A}}_1\langle e^{-ip_*^{(1)}\eta(x_3-d)}\rangle \bar{\mathbf{q}}_1^\infty - i\eta^{-1}\bar{\mathbf{A}}_1\langle e^{-ip_*^{(1)}\eta(x_3-d)}\rangle \bar{\mathbf{q}}_1 \\
\tilde{\mathbf{t}}_1(y_1, y_2, x_3) &= \bar{\mathbf{B}}_1\langle e^{-ip_*^{(1)}\eta(x_3-d)}\rangle \bar{\mathbf{q}}_1^\infty - \bar{\mathbf{B}}_1\langle e^{-ip_*^{(1)}\eta(x_3-d)}\rangle \bar{\mathbf{q}}_1 \\
\tilde{\mathbf{s}}_1(y_1, y_2, x_3) &= \bar{\mathbf{C}}_1\langle e^{-ip_*^{(1)}\eta(x_3-d)}\rangle \bar{\mathbf{q}}_1^\infty - \bar{\mathbf{C}}_1\langle e^{-ip_*^{(1)}\eta(x_3-d)}\rangle \bar{\mathbf{q}}_1
\end{aligned} \tag{26}$$

For $x_3 < 0$ (in material 2):

$$\tilde{\mathbf{u}}_2(y_1, y_2, x_3) = i\eta^{-1}\mathbf{A}_2\langle e^{-ip_*^{(2)}\eta x_3}\rangle\mathbf{q}_2$$

$$\tilde{\mathbf{t}}_2(y_1, y_2, x_3) = \mathbf{B}_2\langle e^{-ip_*^{(2)}\eta x_3}\rangle\mathbf{q}_2 \qquad (27)$$

$$\tilde{\mathbf{s}}_2(y_1, y_2, x_3) = \mathbf{C}_2\langle e^{-ip_*^{(2)}\eta x_3}\rangle\mathbf{q}_2$$

where again, subscripts 1 and 2 denote the quantities in materials 1 and 2, respectively and

$$\mathbf{q}_1^\infty = \mathbf{A}_1^T\mathbf{f} \qquad (28)$$

The complex vectors $\bar{\mathbf{q}}_1$ and $\bar{\mathbf{q}}_2$ in equations (25)-(27) are determined by

$$\bar{\mathbf{q}}_1 = \mathbf{G}_1\langle e^{ip_*^{(1)}\eta d}\rangle\mathbf{A}_1^T\mathbf{f}$$

$$\mathbf{q}_2 = \mathbf{G}_2\langle e^{ip_*^{(1)}\eta d}\rangle\mathbf{A}_1^T\mathbf{f} \qquad (29)$$

$$\mathbf{G}_1 = -\bar{\mathbf{A}}_1^{-1}(\bar{\mathbf{M}}_1 + \mathbf{M}_2)^{-1}(\mathbf{M}_1 - \mathbf{M}_2)\mathbf{A}_1$$

$$\mathbf{G}_2 = -\mathbf{A}_1^{-1}(\bar{\mathbf{M}}_1 + \mathbf{M}_2)^{-1}(\mathbf{M}_1 + \bar{\mathbf{M}}_1)\mathbf{A}_1 \qquad (30)$$

where $\mathbf{M}_\alpha$ are the extended impedance tensors defined as

$$\mathbf{M}_\alpha = -i\mathbf{B}_\alpha\mathbf{A}_\alpha^{-1} \quad (\alpha = 1, 2) \qquad (31)$$

Equations (25)-(27) are the anisotropic magneto-electro-elastic bimaterial Green's displacements and stresses in the Fourier transformed domain. These Green's functions share the same important features as their purely elastic and/or piezoelectric counterparts with details being found in [5,6].

Bimaterial Green's functions in the physical domain

Having obtained the Green's functions in the transformed domain, we now apply the inverse Fourier transforms to equations (25)-(27). To handle the double infinite integrals, the polar coordinate transform is introduced so that the infinite integral with respect to the radial variable can be carried out exactly [5,6]. Thus, the final bimaterial Green's functions in the physical domain can be expressed in terms of regular line-integrals over $[0, 2\pi]$. In the following, we will use only the extended displacement solution in region $x_3 > d$ of material 1 to illustrate the derivation.

Applying the Fourier inverse transform, the extended Green's displacement in equation (25) becomes

$$\mathbf{u}_1(x_1, x_2, x_3) = -\frac{i}{4\pi^2} \int \int \{\eta^{-1}\bar{\mathbf{A}}_1 \langle e^{-i\bar{p}_*^{(1)}\eta(x_3-d)}\rangle \bar{\mathbf{q}}_1^\infty e^{-i(x_1y_1+x_2y_2)}\}dy_1 dy_2$$
$$- \frac{i}{4\pi^2} \int \int \{\eta^{-1}\bar{\mathbf{A}}_1 \langle e^{-i\bar{p}_*^{(1)}\eta x_3}\rangle \bar{\mathbf{q}}_1 e^{-i(x_1y_1+x_2y_2)}\}dy_1 dy_2 \tag{32}$$

The first integral in equation (32) corresponds to the extended Green's displacement in the full space, which in an explicit form, will be derived in the Appendix A. Consequently, the inverse transform needs to be carried out only for the second regular integral, or the complementary part. The singularities involved in the bimaterial Green's function appear only in the full-space solution, which can be evaluated easily because of its explicit-form expression. Denoting the full-space Green's function by $\mathbf{u}_1^\infty(x_1, x_2, x_3)$ and introducing a polar coordinate transform consistent with the one defined in equation (11), i.e.,

$$\begin{bmatrix} y_1 \\ y_2 \end{bmatrix} = \eta \begin{bmatrix} \cos\theta \\ \sin\theta \end{bmatrix} \tag{33}$$

equation (32) is then reduced to [5,6]

$$\mathbf{u}_1(x_1, x_2, x_3) = \mathbf{u}_1^\infty(x_1, x_2, x_3)$$
$$- \frac{i}{4\pi^2} \left[\int_0^{2\pi} d\theta \int_0^\infty \bar{\mathbf{A}}_1 \langle e^{-i\bar{p}_*^{(1)}\eta x_3}\rangle \mathbf{G}_1 \langle e^{i p_*^{(1)}\eta d}\rangle e^{-i\eta(x_1\cos\theta+x_2\sin\theta)}\mathbf{A}_1^T d\eta \right] \mathbf{f} \tag{34}$$

Since the matrices $\mathbf{A}_1$ and $\mathbf{G}_1$ are independent of the radial variable η, the integral with respect to η can actually be performed analytically. Assuming that $x_3 \neq 0$ or $d \neq 0$, equation (34) can be reduced to a compact form

$$\mathbf{u}_1(x_1, x_2, x_3) = \mathbf{u}_1^\infty(x_1, x_2, x_3) + \frac{1}{4\pi^2} \left[\int_0^{2\pi} \bar{\mathbf{A}}_1 \mathbf{G}_u^{(1)} \mathbf{A}_1^T d\theta \right] \mathbf{f} \tag{35}$$

where

$$(\mathbf{G}_u^{(1)})_{IJ} = \frac{(\mathbf{G}_1)_{IJ}}{-\bar{p}_I^{(1)} x_3 + p_J^{(1)} d - (x_1\cos\theta + x_2\sin\theta)} \tag{36}$$

Using a similar procedure, all other bimaterial Green's function components can be derived and they share similar structures as those in [5,6].

It is very interesting that these physical-domain Green's functions possess all the important characteristics as observed and discussed in [5,6] for the purely elastic and/or piezoelectric materials. Furthermore, noticing the following relations of the involved functions

$$P_J(\theta + \pi) = -\bar{P}_J(\theta), \ \mathbf{G}_1(\theta + \pi) = -\bar{\mathbf{G}}_1(\theta), \ \mathbf{G}_2(\theta + \pi) = \bar{\mathbf{G}}_2(\theta)$$
$$\mathbf{A}(\theta + \pi) = \gamma\bar{\mathbf{A}}(\theta), \ \mathbf{B}(\theta + \pi) = -\gamma\bar{\mathbf{B}}(\theta), \ \mathbf{C}(\theta + \pi) = -\gamma\bar{\mathbf{C}}(\theta), \ \gamma = \pm\sqrt{-1} \tag{37}$$

the regular integral over $[0, 2\pi]$ can actually be reduced to the interval of $[0, \pi]$. That is

$$\int_0^{2\pi} g(\theta)d(\theta) = 2\int_0^{\pi} g(\theta)d(\theta) \tag{38}$$

where $g(\theta)$ stands for the integrands in equation (35) and other similar expressions. Therefore, the regular line integral is actually over the interval $[0, \pi]$, a simplification not stated in the author's previous papers [5,6].

Numerical validations and results

The Green's functions derived above are evaluated numerically for three domain cases: a full space, a half space, and two half spaces welded together (i.e. the bimaterial case). For the full space, half space, and material 1 of the bimaterial case (i.e., $z > 0$), material property #1 in Appendix B is used. This is a fully coupled magneto-electro-elastic material with the elastic and piezoelectric properties being those of the piezoelectric material $BaTiO_3$ and the piezomagnetic coefficients q_{ijk} being taken from the magnetostrictive $CoFe_2O_4$ [9]. For material 2 of the bimaterial case ($z < 0$), the elastic and piezoelectric properties are taken from Tiersten [25] as studied in Pan and Yuan [6] (where C_{66} in equation (52a) of [6] should be $.2901 \times 10^{11} N/m^2$, instead of $.6881 \times 10^{11} N/m^2$). Again, the piezomagnetic coefficients q_{ijk} are taken from the magnetostrictive $CoFe_2O_4$. The compound and fully coupled magneto-electro- elastic material properties are listed in material property #2 of Appendix B. We point out that the magnetic permeability of $CoFe_2O_4$ was not used since this material system does not possess a positive internal energy, a special material case, to which the Stroh formalism cannot be applied directly. For the full-space and half-space domain cases, we have also studied three uncoupled material cases by setting the appropriate coefficients to zero: uncoupled E ($e_{ijk} = 0$), uncoupled M ($q_{ijk} = 0$), and uncoupled $E\&M$ ($e_{ijk} = 0$ and $q_{ijk} = 0$), with the last one corresponding to the purely elastic material case. For simplicity, the source is at $(0, 0, 1m)$ and field point at $(1m, 1m, 0)$.

First, a homogeneous full-space is considered, which corresponds to the special case of the bimaterial domain with identical material properties in both materials 1& 2. For this example, the extended Green's displacement tensor is symmetric, and its components can be obtained using either the full-space Green's function formulation derived in Appendix A or the bimaterial Green's function formulation derived in the previous sections. The upper diagonal elements of the extended Green's displacement tenor is listed in Table 1 for the fully coupled, uncoupled E, uncoupled M, and uncoupled $E\&M$ cases. While these values are calculated using the bimaterial Green's functions, use of the full-space Green's function formulation predicts exactly the same results, a mutual validation for both formulations. In Table 1, the units for the elastic displacement, electric and magnetic potentials are, respectively, in m, V, and C/s, and the symbol $G(I, J) \equiv GIJ \equiv G_{IJ}$ (also

G(J,K)	Fully coupled	Uncoupled E	Uncoupled M	Uncoupled E& M
11	.77141370D-12	.78081031D-12	.78459933D-12	.79088298D-12
12	.12027080D-12	.12111470D-12	.12594492D-12	.12594685D-12
13	-.12945921D-12	-.14565674D-12	-.11570894D-12	-.13140542D-12
14	-.10347228D-03	0	-.81376035D-04	0
15	.42667071D-05	.35719554D-05	0	0
22	.77141370D-12	.78081031D-12	.78459933D-12	.79088298D-12
23	-.12945921D-12	-.14565674D-12	-.11570894D-12	-.13140542D-12
24	-.10347228D-03	0	-.81376035D-04	0
25	.42667071D-05	.35719554D-05	0	0
33	.48476833D-12	.55954057D-12	.65390573D-12	.81010088D-12
34	.50073977D-03	0	.69481903D-03	0
35	.24195755D-04	.28451440D-04	0	0
44	-.34041791D+07	-.39412178D+07	-.31760803D+07	-.39412178D+07
45	.29749049D+05	0	0	0
55	-.41918948D+04	-.39092089D+04	-.71176254D+04	-.71176254D+04

Table 1. Extended full-space Green's displacements (GJK) for fully coupled,
uncoupled E, uncoupled M, and uncoupled E& M cases.

G(J,K)	1	2	3	4	5
1	.75107886D-12	.10584332D-12	-.14132043D-12	-.16744449D-03	.26381771D-05
2	.11722656D-12	.77694302D-12	-.16891521D-12	-.17971243D-03	.16147431D-05
3	-.15147253D-12	-.14640169D-12	.54109984D-12	.41179985D-03	.26361567D-04
4	.82068510D-04	.88103967D-04	.54025937D-03	-.69423456D+07	.33367301D+05
5	.55855031D-05	.33664248D-05	.26679164D-04	.39145681D+05	-.38576408D+04

Table 2. Extended Green's displacements (GJK) for fully coupled bimaterial case.

in Table 2 and Figures 2 & 4) denotes the Green's displacement in the I-direction caused by a point force in the J-direction.

Table 1 shows that, in general, the magneto-electro-elastic properties have an apparent influence upon all the Green's displacement components. As an illustration, Figure 2 displays the variation of some of the Green's displacement components with different coupling cases (cases 1, 2, 3, and 4 represent, respectively, the fully coupled, uncoupled E, uncoupled M, and uncoupled $E\&M$ cases). To plot them in the same figure, the Green's components G11, G33, G44, and G55 have been normalized, respectively, by the factor 10^{-12}, 10^{-12}, -10^{7}, and -10^{4}. As can be clearly observed from this figure, the displacements G33 and G55 vary dramatically for different cases, with the maximum difference reaches as high as 45%, a remarkable result that should be of great interest to the smart material analysis and design.
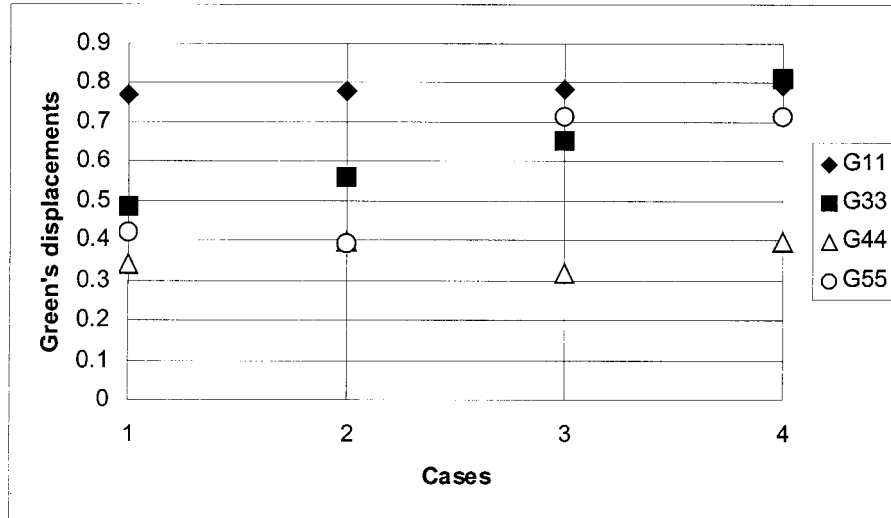
Figure 2.
Variation of normalized full-space Green's displacements versus different coupling cases. Cases 1, 2, 3, and 4 denote, respectively, fully coupled, uncoupled E, uncoupled M, and uncoupled E & M cases.

The magneto-electro-elastic coupling can also have a great effect upon the Green's stresses. For example, Figure 3 shows the variation of the stress component σ_{11} with different cases. The symbols S11, S12, and S13 denote the stress component σ_{11} due to a point force in the 1-, 2-, and 3-directions, respectively. Similar to Figure 2 for the displacements, these stress values are normalized, respectively, by the factor -10^{-2}, -10^{-2}, and 10^{-2}. We observed from this figure that while S11 and S12 vary only slightly with the four cases, the maximum difference for S13 reaches as high as 30%, a magnitude that cannot be ignored during the design procedure.

Having studied the Green's functions in a full space, we now consider the corresponding half space. Since the source is at $(0, 0, 1m)$ and field point at $(1m, 1m, 0)$, the Green's functions represent the surface displacements and stresses caused by a point force interior to the half space. In Figures 4 and 5, the same Green's components studied for the full-space case are plotted using the same normalization factors. It is of particular interest to compare Figure 4 to Figure 2 and Figure 5 to Figure 3. First, for the uncoupled E, uncoupled M, and uncoupled E& M cases, the electric and magnetic potentials (i.e., G44 and G55) on the surface of the half space are exactly twice of those in the corresponding full space, a well-known result from the potential theory. Secondly, except for G33, all other diagonal displacement components (i.e., G11=G22, G44, and G55) on the surface of the half space are also about twice of those in the corresponding full space, irrespective
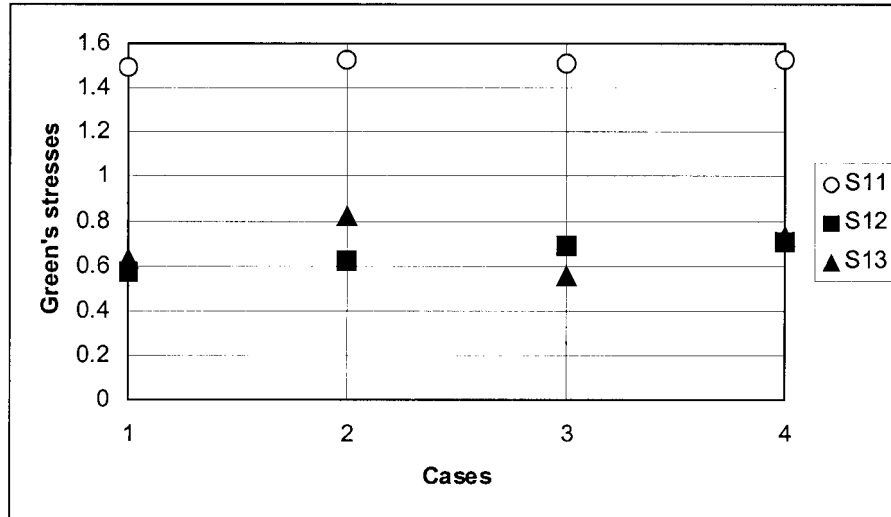
Figure 3.
Variation of normalized full-space Green's stresses versus different coupling cases. Cases 1, 2, 3, and 4 denote, respectively, fully coupled, uncoupled E, uncoupled M, and uncoupled E & M cases.

of the material coupling cases. The third observation comes from the comparison of Figure 5 to Figure 3 where the effect of the traction-free boundary condition on the in-plane stresses is very prominent, resulting in a great variation of these stresses with different coupling cases. For instance, for the full-space case, only S13 has a maximum variation of 30% for different coupling cases; for the half-space case, however, all of their variations (S11, S12, S13) are over 30% (Figure 5). In particular, the magnitude difference of S13 (i.e. σ_{11} due to the z-direction point force) reaches 45%, revealing that the effect of a free surface on the Green's functions can be equally important as the material coupling does. As a third and final example, we discuss the Green's displacements in fully coupled magneto-electro-elastic bimaterials. Again, as for the full-space and half-space cases, the source is at $(0, 0, 1m)$ in material 1 and the field point at $(1m, 1m, 0)$ on the interface. For materials 1 $(z > 0)$ and 2 $(z < 0)$, the material properties #1 and #2 of Appendix B are used, respectively. We briefly remark that, while material property #1 is transversely isotropic, material property #2 is generally anisotropic. Table 2 lists the bimaterial Green's displacements at the interface, with the same units as those in Table 1. Clearly, unlike the full-space Green's displacement tensor, the bimaterial (as well as half-space) Green's tensor is no longer symmetric. The effect of material differences on the Green's displacements can be recognized by comparing the bimaterial displacements to the second column in Table 1. Since the bimaterial Green's functions (especially when the source and field points are both close to
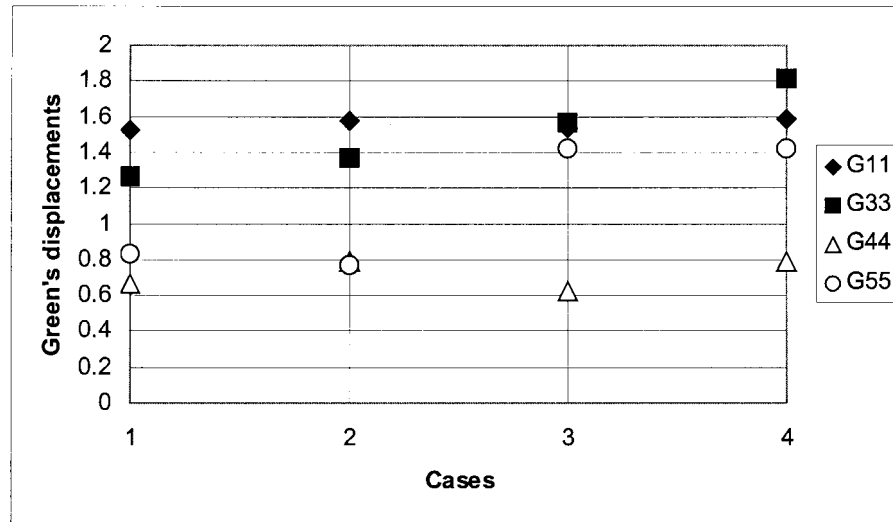
Figure 4.
Variation of normalized half-space Green's displacements versus different coupling cases. Cases 1, 2, 3, and 4 denote, respectively, fully coupled, uncoupled E, uncoupled M, and uncoupled E & M cases.

the interface) are complicated functions of the magneto-electro-elastic coupling, analysis for them needs to be carried out case by case, this will be addressed in the near future.

Conclusions

In this paper, three-dimensional Green's functions in anisotropic magneto-electro-elastic full space, half space, and bimaterials are derived. While for the full space case, the Green's functions are obtained in an explicit form using the Radon transform, the Stroh formalism, and the Cauchy residue theorem, those in the half space and bimaterials are expressed as a sum of the full-space Green's function and a Mindlin-type complementary part, with the latter being evaluated in terms of a regular line integral over $[0, \pi]$. In seeking the full space and the complementary part solutions, the extended Stroh formalism have been used, which further shows that the Stroh formalism is very elegant and powerful. Introduction of the Mindlin's superposition method (full-space solution plus a complementary part) is to handle the singularities of the bimaterial Green's functions so that the involved singularities appear only in the full-space Green's function that can be evaluated accurately using its explicit form expression (without numerical integral!). Since the complementary part of the bimaterial Green's functions is a regular line-
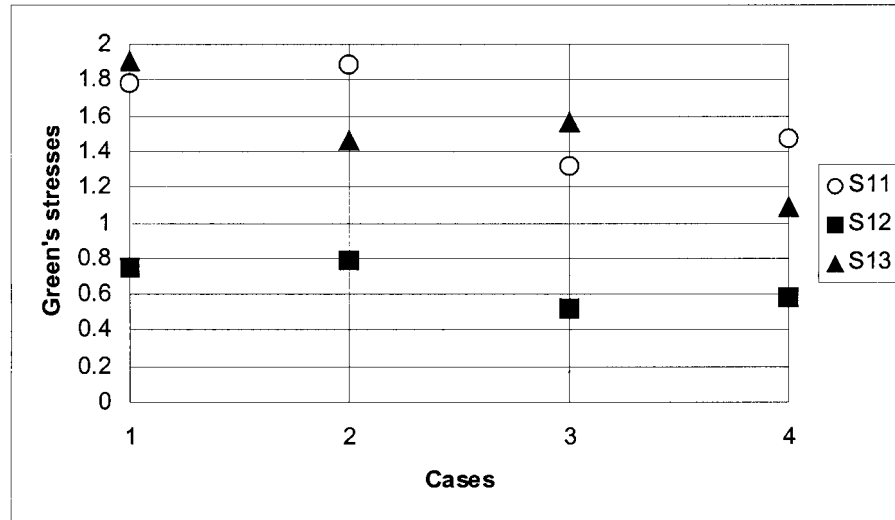
Figure 5.
Variation of normalized half-space Green's stresses versus different coupling cases. Cases 1, 2, 3, and 4 denote, respectively, fully coupled, uncoupled E, uncoupled M, and uncoupled E & M cases.

integral, it can be easily carried out by the regular numerical Gauss quadrature. While the derivatives of the complementary part of the Green's functions with respect to either the source or field point can be carried out exactly under the line integral, those of the full-space Green's functions are evaluated using a very simply, yet accurate difference formulae. Some important features related to the full-space, half-space, and bimaterial Green's functions have been discussed.

Numerical examples are also presented for full-space, half-space, and bimaterial domains with fully coupled, and uncoupled anisotropic magneto-electro-elastic material properties. For the given material properties, the piezoelectric and piezomagnetic effect on the Green's displacements was observed and discussed. For the given source and field points and material properties, we have noticed that the coupling effect of magnetoelectricity on the elastic Green's displacements can be as high as 40%. This remarkable phenomenon has never been reported before.

While the Green's functions derived in this paper can have direct applications to some micromechanics-related problems (opening, inclusion, eigenstrain, etc.) in the smart material and composite material designs, relatively complicated structure problems can be solved using the boundary integral equation method with the current solutions being served as the integral kernels. A primary study of the fracture mechanics problems in 2D anisotropic piezoelectric media using a new pair of BEM formulations has been reported [4].

Acknowledgements

Appendix A

In this Appendix, we derive, for the first time, the explicit Green's functions (extended displacements and stresses) in an anisotropic magneto-electro-elastic full-space. We first derive the integral expression in terms of the Radon transform and the generalized Stroh formalism. This integral will then be carried out by the Cauchy residue theorem. We mention that the method proposed in [20] can also be followed and extended to derive the three-dimensional, anisotropic, and magneto-electro-elastic Green's displacements.

Integral expressions for the Green's functions
Let $\delta(\mathbf{x}) = \delta(x_1, x_2, x_3)$ be the Dirac delta function centered at the origin of a space-fixed Cartesian coordinates $(O; x_1, x_2, x_3)$ and δ_{JP} the fifth-rank Kronecker delta. The extended Green's displacements (a 5×5 tensor $G_{KP}(\mathbf{x})$) are the fundamental solutions of equation (1) caused by an extended point force. Mathematically, this Green's tensor is defined by the partial differential equations:

$$C_{iJKl}G_{KP,li}(\mathbf{x}) = -\delta_{JP}\delta(\mathbf{x}) \qquad (A1)$$

While the first index, K, of the Green's tensor denotes the component of the extended displacement, the second, P, denotes the direction of the extended point force. Since this Green's tensor is generally full for an anisotropic magneto-electro-elastic solid, the elastic, electric, and magnetic fields are thus coupled together. That is, a body force will induce an electric or magnetic potential and an electric or magnetic charge will generate an elastic displacement.

To derive the Green's tensor, we resort to the following plane representation of the Dirac delta function [26,27]

$$\delta(\mathbf{x}) = -\frac{1}{8\pi^2}\Delta \int_\Omega \frac{\delta(\mathbf{n} \cdot \mathbf{x})}{|\mathbf{n}|^2} d\Omega(\mathbf{n}) \qquad (A2)$$

where $\mathbf{n}$ is a vector variable with components (n_1, n_2, n_3) in the space-fixed coordinates $(O; x_1, x_2, x_3)$, $\Omega(\mathbf{n})$ is a closed surface enclosing the origin; The integral is taken over all planes defined by $\mathbf{n} \cdot \mathbf{x} = 0$; The dot '·' denotes the dot product, and Δ is the 3D Laplacian operator.

We now introduce a 5×5 matrix

$$\Gamma_{JK}(\mathbf{n}) = C_{iJKq}n_i n_q \qquad (A3)$$

and denote its inverse by $\Gamma_{JK}^{-1}(\mathbf{n})$. Integrating $\Gamma_{JK}^{-1}(\mathbf{n})\delta(\mathbf{n}\cdot\mathbf{x})$ with respect to $\mathbf{n}$, taking its second derivatives with respect to x_i, and multiplying the result by the extended stiffness matrix C_{iJKq}, we then arrive at the following important identity [27]:

$$C_{iJKq}\frac{\partial^2}{\partial x_i \partial x_q}\int_{\Omega}\Gamma_{JK}^{-1}(\mathbf{n})\delta(\mathbf{n}\cdot\mathbf{x})d\Omega(\mathbf{n}) = \delta_{JP}\Delta\int_{\Omega}\frac{\delta(\mathbf{n}\cdot\mathbf{x})}{|\mathbf{n}|^2}d\Omega(\mathbf{n}) \qquad (A4)$$

Making use of the plane representation (A2), this equation can be rewritten as

$$C_{iJKq}\frac{\partial^2}{\partial x_i \partial x_q}\int_{\Omega}\Gamma_{JK}^{-1}(\mathbf{n})\delta(\mathbf{n}\cdot\mathbf{x})d\Omega(\mathbf{n}) = -8\pi^2\delta_{JP}\delta(\mathbf{x}) \qquad (A5)$$

Comparing equation (A5) to (A1), we finally obtain the following integral expression for the extended Green's displacement tensor

$$G_{JK}(\mathbf{x}) = \frac{1}{8\pi^2}\int_{\Omega}\Gamma_{JK}^{-1}(\mathbf{n})\delta(\mathbf{n}\cdot\mathbf{x})d\Omega(\mathbf{n}) \qquad (A6)$$

or,

$$G_{JK}(\mathbf{x}) = \frac{1}{8\pi^2}\int_{\Omega}\frac{A_{JK}(\mathbf{n})}{D(\mathbf{n})}\delta(\mathbf{n}\cdot\mathbf{x})d\Omega(\mathbf{n}) \qquad (A7)$$

where $A_{JK}(\mathbf{n})$ and $D(\mathbf{n})$ are, respectively, the adjoint matrix and determinant of $\Gamma_{JK}(\mathbf{n})$. This integral expression of the Green's function is quite general and contains previous results in anisotropic elastic and piezoelectric spaces as its special cases.

Explicit expressions for Green's functions
The integral expression (A7) for the Green's tensor can actually be transformed to a 1D infinite integral and the result can then be reduced to a summation of five residues. This is achieved by expressing the vector variable $\mathbf{n}$ in terms of a new, orthogonal, and normalized system $(O; \mathbf{e}, \mathbf{p}, \mathbf{q})$, instead of the space-fixed Cartesian coordinates $(O; x_1, x_2, x_3)$. The new base $(\mathbf{e}, \mathbf{p}, \mathbf{q})$ are chosen as the following

$$\mathbf{e} = \mathbf{x}/r; \quad r = |\mathbf{x}| \qquad (A8)$$

Now, let $\mathbf{v}$ be an arbitrary unit vector different from $\mathbf{e}$ ($\mathbf{v} \neq \mathbf{e}$), the two unit vectors orthogonal to $\mathbf{e}$ can then be selected as:

$$\mathbf{p} = \frac{\mathbf{e}\times\mathbf{v}}{|\mathbf{e}\times\mathbf{v}|}; \quad \mathbf{q} = \mathbf{e}\times\mathbf{p} \qquad (A9)$$

It should be emphasized that $\mathbf{e} \neq \mathbf{v}$ should be normalized so that $\mathbf{p}$ is a unit vector.

In the new reference system $(O; \mathbf{e}, \mathbf{p}, \mathbf{q})$, we let the vector variable $\mathbf{n}$ be expressed as

$$\mathbf{n} = \xi\mathbf{p} + \zeta\mathbf{q} + \eta\mathbf{e} \tag{A10}$$

It is clear then that

$$\mathbf{n} \cdot \mathbf{x} = \mathbf{p} \cdot \mathbf{x}\xi + \mathbf{q} \cdot \mathbf{x}\zeta + \mathbf{e} \cdot \mathbf{x}\eta = r\eta \tag{A11}$$

Therefore, in terms of the reference system $(O; \mathbf{e}, \mathbf{p}, \mathbf{q})$, equation (A7) becomes

$$G_{JK}(\mathbf{x}) = \frac{1}{8\pi^2} \int_\Omega \frac{A_{JK}(\xi\mathbf{p} + \zeta\mathbf{q} + \eta\mathbf{e})}{D(\xi\mathbf{p} + \zeta\mathbf{q} + \eta\mathbf{e})} \delta(r\eta) d\Omega(\xi, \zeta, \eta) \tag{A12}$$

where Ω is again a closed surface enclosing the origin $(\xi, \zeta, \eta) = (0, 0, 0)$.

Carrying out the integration of (A12) with respect to η yields [26,27]

$$G_{JK}(\mathbf{x}) = \frac{1}{4\pi^2 r} \int_{-\infty}^{\infty} \frac{A_{JK}(\mathbf{p} + \zeta\mathbf{q})}{D(\mathbf{p} + \zeta\mathbf{q})} d\zeta \tag{A13}$$

We now look at the matrix $\Gamma_{JK}(\mathbf{p} + \zeta\mathbf{q})$ and its determinant $D(\mathbf{p} + \zeta\mathbf{q})$. It turns out that the matrix Γ_{JK} can actually be expressed by the Stroh formalism. That is,

$$\Gamma(\mathbf{p} + \zeta\mathbf{q}) \equiv \mathbf{Q} + \zeta(\mathbf{R} + \mathbf{R}^T) + \zeta^2\mathbf{T} \tag{A14}$$

where

$$Q_{IK} = C_{jIKs}p_j q_s, \quad R_{IK} = C_{jIKs}p_j q_s, \quad T_{IK} = C_{jIKs}q_j q_s \tag{A15}$$

The determinant $D(\mathbf{p} + \zeta\mathbf{q})$ is a tenth-order polynomial equation of ζ and has ten roots. For the materials studied in this paper, five of them are the conjugate of the remainder. These roots can be found either by expanding the determinant $D(\mathbf{p} + \zeta\mathbf{q})$ into the polynomial, or by finding the ten eigenvalues of the following linear eigenequation [3]

$$\begin{bmatrix} \mathbf{N}_1 & \mathbf{N}_2 \\ \mathbf{N}_3 & \mathbf{N}_1^T \end{bmatrix} \begin{bmatrix} \mathbf{a} \\ \mathbf{b} \end{bmatrix} = \zeta \begin{bmatrix} \mathbf{a} \\ \mathbf{b} \end{bmatrix} \tag{A16}$$

where

$$\mathbf{N}_1 = -\mathbf{T}^{-1}\mathbf{R}^T, \ \mathbf{N}_2 = \mathbf{T}^{-1}, \ \mathbf{N}_3 = \mathbf{R}\mathbf{T}^{-1}\mathbf{R}^T - \mathbf{Q} \tag{A17}$$

and the eigenvectors $\mathbf{a}$ and $\mathbf{b}$ are the coefficients of the extended displacement and traction vectors.

Assume that

$$\text{Im}\zeta_m > 0; m = 1, 2, 3, 4, 5$$

and ζ_m^* is the conjugate of ζ_m, the extended Green's displacement can be finally expressed explicitly as

$$G_{JK}(\mathbf{x}) = -\frac{\mathrm{Im}}{2\pi r} \sum_{m=1}^{5} \frac{A_{JK}(\mathbf{p} + \zeta_m \mathbf{q})}{a_{11}(\zeta_m - \zeta_m^*) \prod_{\substack{k=1 \\ k \neq m}}^{5} (\zeta_m - \zeta_k)(\zeta_m - \zeta_k^*)} \tag{A18}$$

where $a_{11} = \det(\mathbf{T})$ is the coefficient of ζ^{10}.

There are a couple of features associated with this new expression: First of all, equation (A18) is an explicit expression. It can therefore be evaluated very accurately and efficiently. For a given pair of field and source points, we need only to solve a 10th-order linear eigenequations, or a 10th-order polynomial equation numerically once in order to obtain all the components of the extended Green's displacement. Secondly, in obtaining equation (A18), we have assumed that all the poles are simple. Should the poles be multiple, a slight change in the material constants will result in single poles, with negligible errors in the computed Green's tensor [28]. Thirdly, since Γ_{JK} is symmetric, so is its adjoint A_{JK}. Therefore, the extended Green's displacement G_{JK} is symmetric and one needs to calculate only 15 out of its 25 elements. Finally, although one can choose the vector $\mathbf{v}$ ($\neq \mathbf{e}$) arbitrarily, it should be one of the base vectors in the space-fixed Cartesian coordinates, i.e., $(1, 0, 0)$, or $(0, 1, 0)$, or $(0, 0, 1)$. The analytical expression for the extended Green's displacement is much simpler using such a vector $\mathbf{v}$ than using any other vectors.

We have just derived an explicit expression for the extended Green's displacement. In the application of the boundary integral equation and other related methods, one also needs the extended Green's stress, which can be obtained by taking the derivative of the extended Green's displacement. However, an explicit expression for the derivative of the Green's displacement is too complicated to be implemented efficiently. Here, the numerical method recently proposed by Pan and Tonon [27] is used to evaluate these derivatives. It is based on the simple interpretation of the Lagrange polynomials, and yet it turns out to be very efficient and accurate.

Following Pan and Tonon [27], for instance, the derivatives of the Green's tensor G_{PK} with respect to the coordinates at $\mathbf{x} = (x_1, x_2, x_3)$ are evaluated by

$$\frac{\partial G_{PK}}{\partial x_1} \approx \frac{1}{2h} [G_{PK}(x_1 + h, x_2, x_3) - G_{PK}(x_1 - h, x_2, x_3)] \tag{A19}$$

$$\frac{\partial G_{PK}}{\partial x_2} \approx \frac{1}{2h} [G_{PK}(x_1, x_2 + h, x_3) - G_{PK}(x_1, x_2 - h, x_3)] \tag{A20}$$

$$\frac{\partial G_{PK}}{\partial x_3} \approx \frac{1}{2h} [G_{PK}(x_1, x_2, x_3 + h) - G_{PK}(x_1, x_2, x_3 - h)] \tag{A21}$$

where the interval h is chosen as [27]

$$h = r \cdot 10^{-6}$$

with r being the distance between the field and source points.

Appendix B

B1). Material property # 1 (for full space, half space, and material 1 of the bimaterial case)

   1. Elastic constants

$$[C] = \begin{bmatrix} 166 & 77 & 78 & 0 & 0 & 0 \\ & 166 & 78 & 0 & 0 & 0 \\ & & 162 & 0 & 0 & 0 \\ & & & 43 & 0 & 0 \\ & \text{symm.} & & & 43 & 0 \\ & & & & & 44.5 \end{bmatrix} (10^9 \text{N/m}^2$$

   2. Piezoelectric constants

$$[e] = \begin{bmatrix} 0 & 0 & 0 & 0 & 11.6 & 0 \\ 0 & 0 & 0 & 11.6 & 0 & 0 \\ -4.4 & -4.4 & 18.6 & 0 & 0 & 0 \end{bmatrix} (\text{C/m}^2)$$

   3. Dielectric permeability coefficients

$$[\varepsilon] = \begin{bmatrix} 11.2 & 0 & 0 \\ 0 & 11.2 & 0 \\ 0 & 0 & 12.6 \end{bmatrix} (10^{-9}\text{C/Vm})$$

   4. Piezomagnetic constants

$$[q] = \begin{bmatrix} 0 & 0 & 0 & 0 & 550 & 0 \\ 0 & 0 & 0 & 550 & 0 & 0 \\ 580.3 & 580.3 & 699.7 & 0 & 0 & 0 \end{bmatrix} (\text{N/Am})$$

   5. Magnetoelectric coefficients d(i,j)=0 (for i,j=1,3) (in Ns/VC)

6. Magnetic permeability coefficients

$$[\mu] = \begin{bmatrix} 5 & 0 & 0 \\ 0 & 5 & 0 \\ 0 & 0 & 10 \end{bmatrix} (10^{-6}\text{Ns}^2/\text{C}^2)$$

B2). Material property # 2 (for material 2 of the bimaterial case)
1. Elastic constants

$$[C] = \begin{bmatrix} 86.74 & -8.25 & 27.15 & -3.66 & 0 & 0 \\ & 129.77 & -7.42 & 5.7 & 0 & 0 \\ & & 102.83 & 9.92 & 0 & 0 \\ & & & 38.81 & 0 & 0 \\ & \text{symm.} & & & 68.81 & 2.53 \\ & & & & & 29.01 \end{bmatrix} (10^9\text{N/m}^2)$$

2. Piezoelectric constants

$$[e] = \begin{bmatrix} .171 & -.152 & -.0187 & .067 & 0 & 0 \\ 0 & 0 & 0 & 0 & .108 & -.095 \\ 0 & 0 & 0 & 0 & -.0761 & .067 \end{bmatrix} (\text{C/m}^2)$$

3. Dielectric permeability coefficients

$$[\varepsilon] = \begin{bmatrix} 39.21 & 0 & 0 \\ 0 & 39.82 & .86 \\ 0 & .86 & 40.42 \end{bmatrix} (10^{-12}\text{C/Vm})$$

4. Piezomagnetic constants

$$[q] = \begin{bmatrix} 0 & 0 & 0 & 0 & 550 & 0 \\ 0 & 0 & 0 & 550 & 0 & 0 \\ 580.3 & 580.3 & 699.7 & 0 & 0 & 0 \end{bmatrix} (\text{N/Am})$$

5. Magnetoelectric coefficients d(i,j)=0 (for i,j=1,3) (in Ns/VC)
6. Magnetic permeability coefficients

$$[\mu] = \begin{bmatrix} 5 & 0 & 0 \\ 0 & 5 & 0 \\ 0 & 0 & 10 \end{bmatrix} (10^{-6}\text{Ns}^2/\text{C}^2)$$

References

[1] Nan, C. W., Magnetoelectric effect in composites of piezoelectric and piezomagnetic phases. *Physical Review*, **B50** (1994), 6082-6088.

[2] Benveniste, Y., Magnetoelectric effect in fibrous composites with piezoelectric and piezomagnetic phases. *Physical Review* **B51** (1995), 16424-16427.

[3] Ting, T. C. T., *Anisotropic Elasticity*, Oxford University Press, Oxford 1996.

[4] Pan, E., A BEM Analysis of Fracture Mechanics in 2D Anisotropic Piezoelectric Solids, *Engineering Analysis with Boundary Elements* **23** (1999), 67-76.

[5] Pan, E. and Yuan, F. G., Three-dimensional Green's Functions in Anisotropic Bimaterials, *International Journal of Solids and Structures* **37** (2000), 5329-5351.

[6] Pan, E. and Yuan, F. G., Three-dimensional Green's Functions in Anisotropic Piezoelectric Bimaterials, *International Journal of Engineering Science* **38** (2000), 1939-1960.

[7] Bacon, D. J., Barnett, D. M. and Scattergood, R. O., The anisotropic continuum theory of lattice defects. *Progress in Materials Science* **23** (1978), 51-262.

[8] Mura, T., *Micromechanics of Defects in Solids*, 2nd rev. ed. (Kluwer Academic Publ. 1998).

[9] Huang, J. H. and Kuo, W. S., The analysis of piezoelectric/piezomagnetic composite materials containing ellipsoidal inclusions. *J. Appl. Phys.* **81** (1997), 1378-1386.

[10] Huang, J. H., Chiu, Y. H. and Liu, H. K., Magneto-electro-elastic Eshelby tensors for a piezoelectric-piezomagnetic composite reinforced by ellipsoidal inclusions. *J. Appl. Phys.* **83** (1998), 5364-5370.

[11] Huang, J. H., Analytical predictions for the magneto-electric coupling in piezomagnetic materials reinforced by piezoelectric ellipsoidal inclusions. *Physical Review* **B58** (1998), 12-15.

[12] Li, J. and Dunn, M. L., Anisotropic coupled-field inclusion and inhomogeneity problems. *Philosophical Magazine* **A77** (1998a), 1341-1350.

[13] Li, J. and Dunn, M. L., Micromechanics of magnetoelectroelastic composite materials: Average fields and effective behavior. *Journal of Intelligent Material Systems and Structures* **9** (1998b), 404-416.

[14] Ting, T. C. T., Recent developments in anisotropic elasticity, *International Journal of Solids and Structures* **37** (2000), 401-409.

[15] Alshits, V. I., Darinskii, A. N., and Lothe, J., On the existence of surface waves in half-infinite anisotropic elastic media with piezoelectric and piezomagnetic properties. *Wave Motion* **16** 1992), 265-283.

[16] Alshits, V. I., Kirchner, H. O. K. and Ting, T. C. T., Angularly inhomogeneous piezoelectric piezomagnetic magnetoelectric anisotropic media. *Philosophical Magazine Letters* **71** (1995), 285-288.

[17] Chung, M. Y. and Ting, T. C. T., The Green's function for a piezoelectric piezomagnetic magnetoelectric anisotropic elastic medium with an elliptic hole or rigid inclusion. *Philosophical Magazine Letters* **72** (1995), 405-410.

[18] Kirchner, H. O. K. and Alshits, V. I., Elastically anisotropic angularly inhomogeneous media II. The Green's function for piezoelectric, piezomagnetic and magnetoelectric media. *Philosophical Magazine* **A74** (1996), 861-885.

[19] Barnett, D. M. and Lothe, J., Line Force Loadings on Anisotropic Half-Spaces and Wedges, *Physica Norvegica* **8** (1975), 13-22.

[20] Ting, T. C. T. and Lee, V. G., The three-dimensional elastostatic Green's function for general anisotropic linear elastic solids, *Q. J. Mech. Appl. Math.* **50** (1997), 407- 426.

[21] Wu, K. C., Generalization of the Stroh formalism to 3-dimensional anisotropic elasticity, *J. Elasticity* **51** (1998), 213-225.

[22] Mindlin, R. D., Force at a Point in the Interior of a Semi-Infinite Solid, *Physics* **7** (1936), 195-202.

[23] Barnett, D. M. and Lothe, J., Dislocations and Line Charges in Anisotropic Piezoelectric Insulators, *Phys. Stat. Sol. (b)* **67** (1975), 105-111.

[24] Suo, Z., Kuo, C. M., Barnett, D. M., and Willis, J. R., Fracture mechanics for piezoelectric ceramics, *Journal of the Mechanics and Physics of Solids* **40** (1992), 739-965.

[25] Tiersten, H. F., *Linear Piezoelectric Plate Vibrations*, Plenum, New York 1969.

[26] Wang, C. Y., Elastostatic fields produced by a point source in solids of general anisotropy, *J. Eng. Math.* **32** (1997), 41-52.

[27] Pan, E. and Tonon, F., Three-dimensional Green's Functions in Anisotropic Piezoelectric Solids, *International Journal of Solids and Structures* **37** (2000), 943-958.

[28] Tonon, F., Pan, E., and Amadei, B., Green's functions and BEM formulation for 3D anisotropic media, *Computers and Structures* **79** (2001), 469–482.

Ernian Pan
Structures Technology, Inc.
543 Keisler Dr., Suite 204
Cary, North Carolina 27511
USA
e-mail: enianpan@hotmail.com

To access this journal online:
http://www.birkhauser.ch